Available online at www.sciencedirect.com
ScienceDirect
Aerosol Science 39 (2008) 460–466
Journal of Aerosol Science
www.elsevier.com/locate/jaerosci

Technical note

# Charge distributions of aerosol dioctyl sebacate particles charged in a dielectric barrier discharger

Jeong Hoon Byeon[a], Jun Ho Ji[b], Jae Hong Park[a], Ki Young Yoon[a], Jungho Hwang[a,*]

[a] *Department of Mechanical Engineering, Yonsei University, Seoul 120-749, Republic of Korea*
[b] *Division of Digital Appliance Network, Samsung Electronics Co., Ltd., Suwon 442-742, Republic of Korea*

Received 25 October 2007; received in revised form 20 December 2007; accepted 21 December 2007

**Abstract**

The collection efficiencies of submicron aerosol particles using a two-stage, dielectric barrier discharge (DBD) type electrostatic precipitator have been reported previously [Byeon et al. (2006). Collection of submicron particles by an electrostatic precipitator using a dielectric barrier discharge. *Journal of Aerosol Science*, *37*, 1618–1628]. In this paper, the charge distributions of aerosol dioctyl sebacate (DOS) particles, which had a mobility equivalent diameter of 118, 175, and 241 nm and were charged in a DBD charger, were examined using a tandem differential mobility analyzer (TDMA) system at applied voltages of 9–11 kV and frequencies of 60–120 Hz. The mean number of elementary charges for positively or negatively charged particles increased slightly with increasing applied voltage or frequency. However, the number of elementary charges increased significantly with increasing particle size. At any applied voltage and frequency, the charge distributions of these particles of these sizes indicated asymmetric bipolar charging. The positive-to-negative charge ratios were 10.4, 4.7, and 3.0 for particle sizes of 118, 175, and 241 nm, respectively, at a DBD voltage and frequency was 9 kV and 60 Hz, respectively. Fluorometric analysis showed that average positive-to-negative charge ratios were 11.5, 4.9, and 3.7 for particle sizes of 118, 175, and 241 nm, which agrees well with the TDMA results. Further fluorometric analyses with larger particles (514 and 710 nm) and higher frequencies (1 and 2 kHz) showed that the positive-to-negative charge ratio reached almost unity with increasing particle size or frequency.


*Keywords:* Dielectric barrier discharger; Charge distribution; Tandem differential mobility analyzer; Asymmetric bipolar charging; Fluorometric analysis

## 1. Introduction

Aerosol particles can be electrically charged by certain forces with the number of elementary charges on a particle depending on the charging mechanism. Accurate information on the magnitude and distribution of the particle charge is essential for examining the electrostatic effects in many fields of science and technology, e.g. atmospheric physics, aerosol-phase based material synthesis, contamination control, etc. (Borra, 2006; Forsyth, Liu, & Romay, 1998; Maisels, Jordan, & Fissan, 2003; Tsai, Lin, Deshpande, & Liu, 2005). In particular, the particle charge distribution provides a mechanism for the collection of particles using electrostatic precipitation (Duarte Fo, Marra, Kachan, & Coury, 2000; Maricq, 2006).

* Corresponding author. Fax: +82 2 312 2821.
*E-mail address:* hwangjh@yonsei.ac.kr (J. Hwang).

0021-8502/$ - see front matter © 2007 Elsevier Ltd. All rights reserved.
doi:10.1016/j.jaerosci.2007.12.008

The collection efficiencies of submicron aerosol particles using a two-stage, dielectric barrier discharge (DBD) type electrostatic precipitator (ESP) have been reported previously (Byeon et al., 2006). It was reported that the collection efficiencies showed a similar trend to those of a conventional direct current (DC) corona discharger type ESP even though the DBD charger was operated in an AC field. However, there are no reports of the charge distribution of particles exiting the DBD charger. Hence, the role of the charger needs to be clarified.

In this paper, the charge distribution of submicron aerosol particles passing through a DBD charger were examined at applied voltages of 9–11 kV and frequencies of 60–120 Hz. A configuration of a tandem differential mobility analyzer (TDMA), which was used by Alguacil and Alonso (2006), Kwon, Sakurai, Seto, and Kim (2006), Lee, Kim, Shimada, and Okuyama (2005), and Stommel and Riebel (2004), was adopted in this study to detect the number of positive or negative elementary charges of particles. To support the TDMA results, the fluorometric analysis methodology introduced by Sharma and Schulman (1999) was used to measure the ratio of positive-to-negative charged particles. Dioctyl sebacate (DOS) particles, 118, 175, and 241 nm in size, were selected in this study because the TDMA method works best for particles in the 10–200 nm size range (Hinds, 1999) and DOS particles were used by Byeon et al. (2006).

## 2. Experimental

Fig. 1(a) gives a schematic diagram of the TDMA experimental setup. A Collison atomizer and an evaporation–condensation aerosol conditioner (3072, TSI) were used to generate monodisperse spherical aerosol particles (Park, An, & Hwang, 2007). DOS (density = 0.914 g/cm$^3$) particles were generated by atomizing a solution containing DOS (5–40 vol%) mixed with isopropyl alcohol (IPA, 95–60 vol%). The desired DOS particle concentration after the aerosol conditioner was controlled using a laminar flow meter. The TDMA system consisted of two differential electrical mobility analyzers (DMA, 3081, TSI), DMA-1 and DMA-2, and a condensation particle counter (CPC, 3022A, TSI). DMA-1 and DMA-2 were placed before and after the DBD charger, respectively. DMA-1 and DMA-2 were operated at an aerosol and sheath air flow rate of 0.3 and 3 L/min, respectively, which created an aerosol-to-sheath ratio of

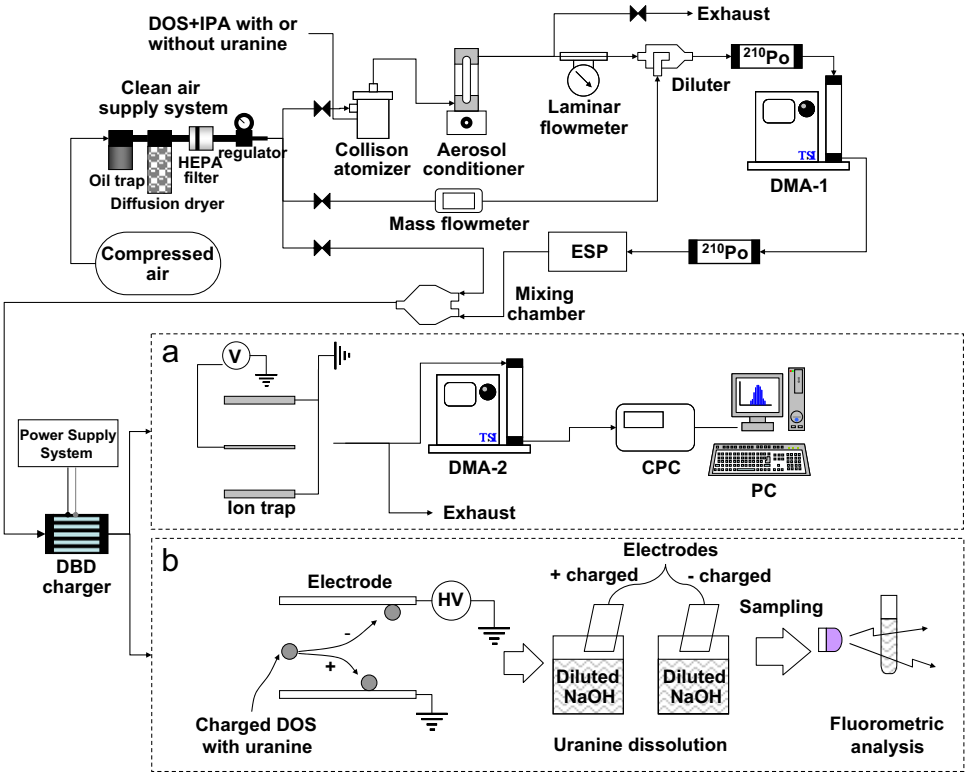


Fig. 1. Schematic diagram showing the (a) TDMA and (b) fluorometric methods.

0.1. The DMA-1 was used as an electrical field classifying system, which was operated at a chosen fixed voltage to extract the particles of equivalent electrical mobility. To insert the monodisperse particles into the DBD charger, the conditioned particles were classified by DMA-1 after passing through a charge neutralizer (Po-210, 2U500, NRD). The particles exiting DMA-1 (all with equivalent electrical mobility) were exposed to another Po-210 neutralizer. The charge redistributed particles were passed through a cylindrical ESP (Ji, Bae, & Hwang, 2004) to remove the charged particles. The ESP consisted of a cylindrical brass housing containing an expander inlet, a central electrode, and a converging nozzle outlet. The ESP was designed to remove both positively and negatively charged particles by applying a high voltage (2 kV) to the central electrode and grounding the housing. The remaining uncharged monodisperse particles were fed into a DBD charger with particle-free air to control the particle residence time in the DBD charger. For an accurate measurement of the charge distribution, the free gaseous ions leaving the charger were removed using an ion trap. Particles from the ion trap were scanned by DMA-2 to measure the charge distribution corresponding to the initially selected mobility diameter. Finally, the particles were counted using a CPC. To detect positively charged particles, the bipolar charged particles from the DBD charger were introduced to DMA-2. DMA-2, which was operated with a negatively charged electrode, selected the positively charged particles of equivalent electrical mobility. The fraction of negatively charged particles was obtained in the same manner by switching the polarity of DMA-2.

Fig. 1(b) shows a schematic diagram of the fluorometric experiments. To generate fluorescent DOS particles, 1 g of uranine (fluorescent material) was added to 100 mL of the DOS-IPA solution (previously used for the TDMA experiments). This mixture solution was aerosolized monodispersely using a similar process to that used for the TDMA experiments. Uncharged monodisperse DOS particles containing uranine were subjected to the DBD charger through the cylindrical ESP. The particles charged in the DBD charger were then introduced into a planar ESP (Byeon et al., 2006) where the positively and negatively charged particles were collected electrostatically on their counter electrodes. The ESP consisted of three parallel copper plate electrodes (a 200 mm streamwise length and an 80 mm spanwise length), two of which were grounded. A high DC voltage (8 kV) was applied to the other electrode (cathode) located in the center. The spacing between the grounded electrode and the cathode was 10 mm. After the charged particles had precipitated, the collecting electrodes were separated from the ESP and immersed into 100 mL of a 0.017 N NaOH (sodium hydroxide) solution. The uranine containing particles collected on the positively or negatively charged electrode were dissolved in a NaOH solution for 10 min. A sample of the mixture was placed in a 3 mL cell for fluorometric analysis. In fluorometric analysis, the sample was first excited from its ground electronic state (a low energy state) to one of the various vibrational states in the excited electronic state (a high energy state) by absorbing a photon of light. The excitation spectrum was measured by recording the sum of fluorescent light emitted at all frequencies as function of the frequency of monochromatic incident light. A fluorometer (Turner Quantech (Barnstead)) used bandpass filters to attenuate the excitation and detection beams, with a source radiation wavelength of 360–390 nm and a detection special window of 440–490 nm. A quartz halogen lamp provided the source radiation and a photomultiplier tube was used for detection.

## 3. Results and discussion

The ion trap voltage was selected as 140 V where particle loss to the trap was less than 2%.

Fig. 2 shows electrical mobility distributions and charge spectra measured by DMA-2 when the applied voltage and frequency were 9 kV and 60 Hz, respectively. The experiments were carried out using monodisperse particles, 118 nm in size. The residence time was 0.048 s. The results show that particles, 118 nm in size, were mostly positively charged. Different peaks appearing in Fig. 2 correspond to the different number of charges on the positively or negatively charged particles, respectively. The relative area under each peak gives the fraction of charged particles carrying a certain number of elementary charges. The number of elementary charges of the charged particles was calculated using the following equation:

$$n = Z_{\text{DMA-2}}/Z_{\text{DMA-1}}, \tag{1}$$

where $Z_{\text{DMA-1}}$ and $Z_{\text{DMA-2}}$ are the electrical mobilities (Hinds, 1999) measured by DMA-1 and DMA-2, respectively.

The data shown in Fig. 2 were rearranged in Fig. 3, where the number concentrations of the total particles were measured without using DMA-2. Fig. 3 also shows results when the applied voltage in the DBD charger was increased to 10 or 11 kV. The positive and negative charge distributions were shifted slightly to higher charge values with increasing DBD voltage from 9 to 11 kV. With an ion counter (AIC-2000, Sato Shoji Inc.), concentrations of positive ions and

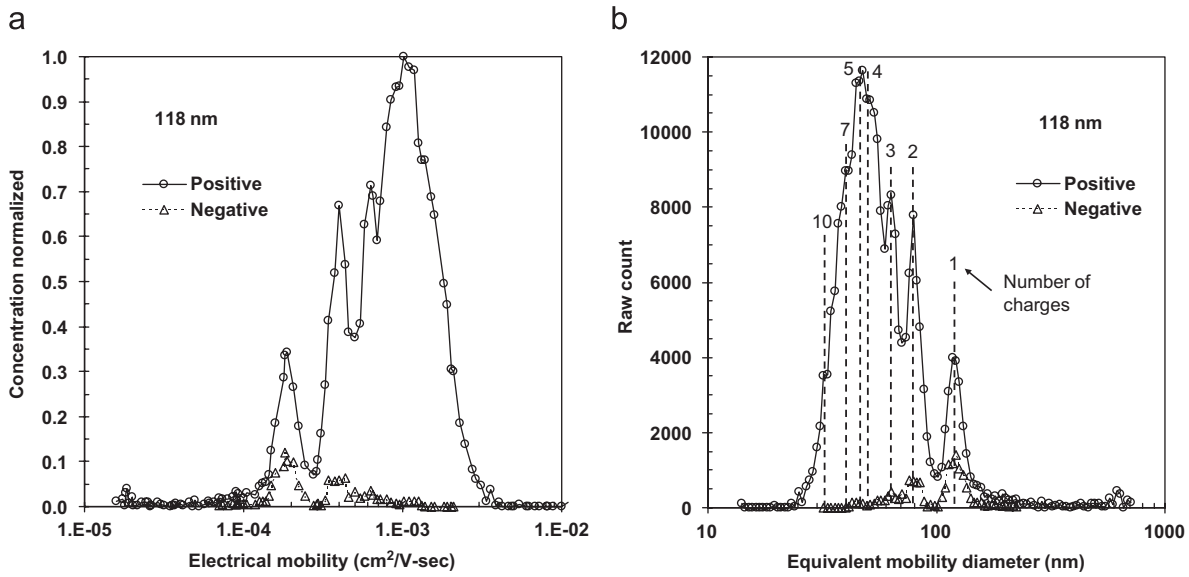


Fig. 2. (a) Electrical mobility distributions and (b) charge spectra of positively and negatively charged particles (DBD: 9 kV, 60 Hz).

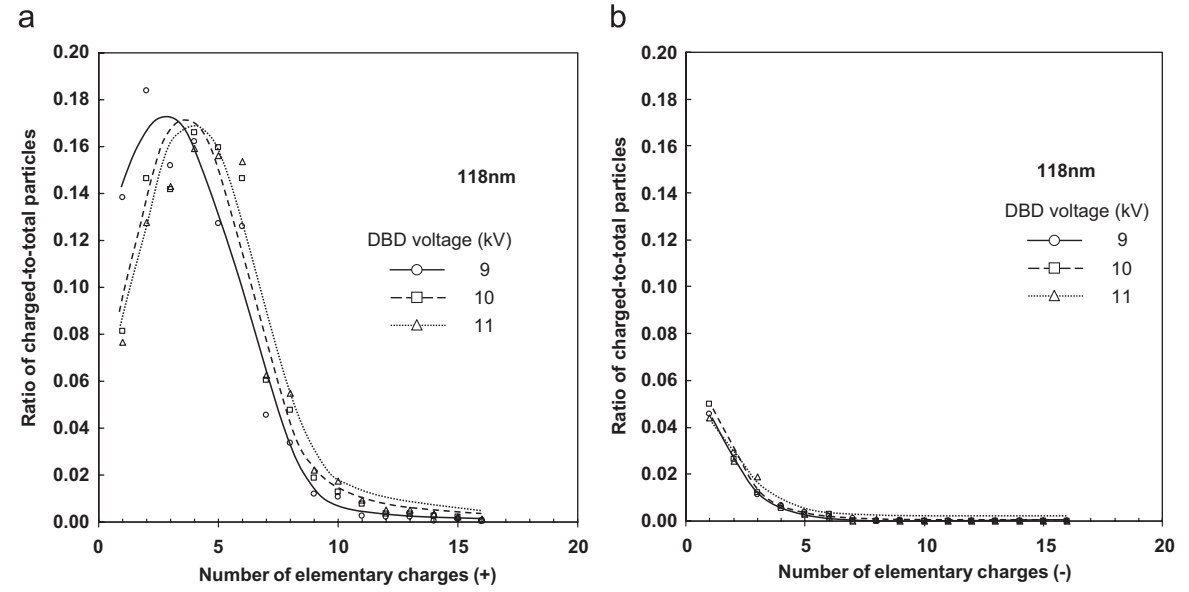


Fig. 3. Distribution of (a) positively and (b) negatively charged particles with the DBD applied voltage (DBD: 60 Hz).

negative ions were measured. The concentrations increased from $1.4 \times 10^6$ to $2.8 \times 10^6$ ions/cm$^3$ and from $0.9 \times 10^5$ to $1.8 \times 10^5$ ions/cm$^3$ for positive ions and negative ions, respectively, when the voltage increased from 9 to 11 kV.

The effect of the DBD frequency was also examined and the results are shown in Fig. 4. Both positive and negative charge distributions slightly shifted to a higher charge values with increasing frequency from 60 to 120 Hz. According to the previous studies, a higher frequency resulted in a higher current and thus a higher ion concentration, (Krupa, Jaworek, Lackowski, Czech, & Luckner, 2005; Lackowski, Adamiak, Jaworek, & Krupa, 2003; Lackowski, Jaworek, & Krupa, 2003). An AC field charger is a device in which the particles are charged by an ionic current and periodically

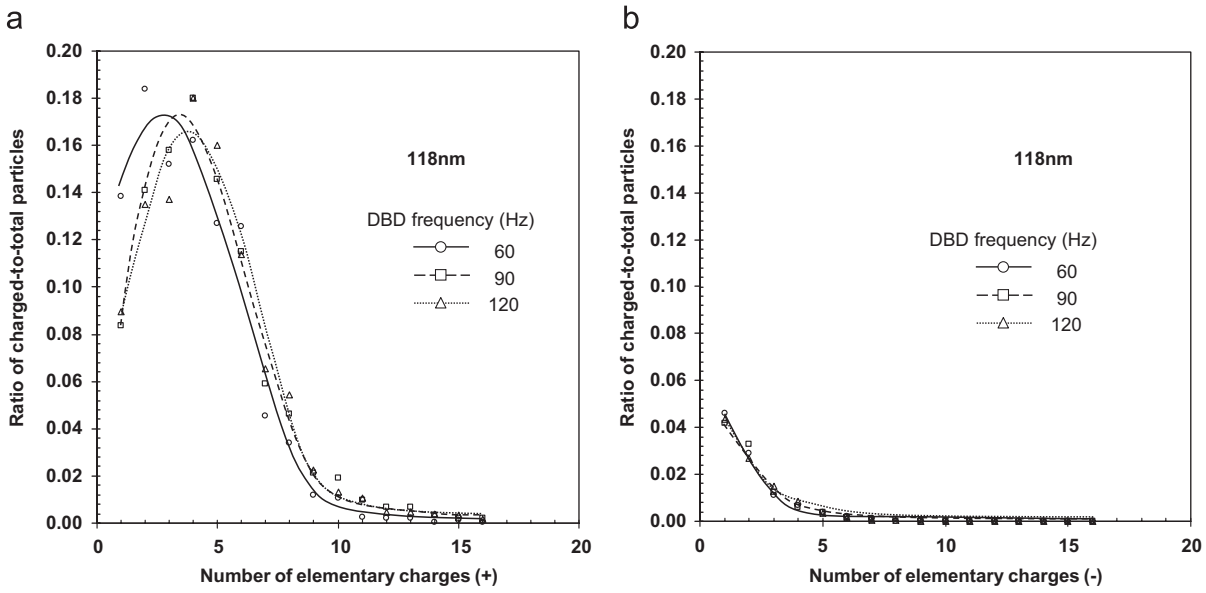


Fig. 4. Distributions of (a) positively and (b) negatively charged particles with frequency (DBD: 9 kV).

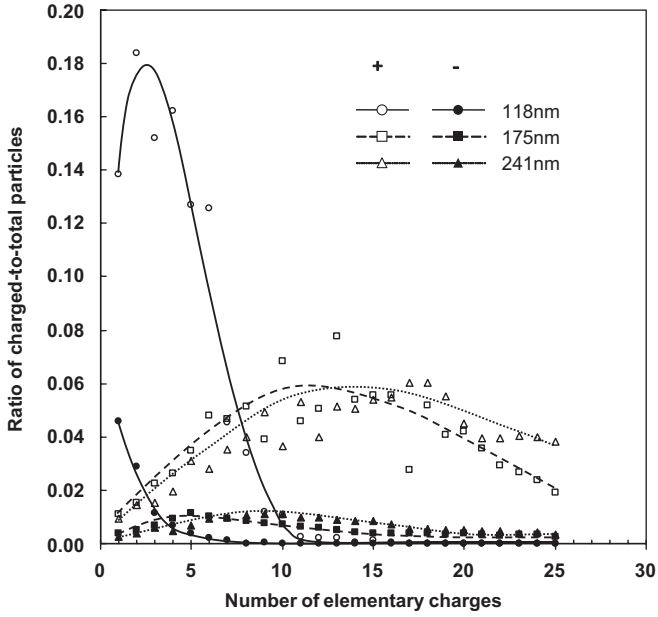


Fig. 5. Charge distributions as function of particle size (DBD: 9 kV, 60 Hz).

deflected by an alternating electric field during their flow through the charger. Byeon et al. (2006) reported that the exposure time of particles to gaseous ions increases with increasing frequency.

Fig. 5 shows the effect of particle size on the positive and negative charge distribution. Both the positive and negative charge distribution were shifted to higher charge values with increasing size from 118 to 241 nm. This was attributed to the increase in charging probability with increasing particle size. Moreover, the results show that the ratio between positive and negative charges decreased with increasing particle size, as discussed in the previous studies (Dhanorkar & Kamra, 2003; Hinds, 1999; Hoppel & Frick, 1986). Table 1 shows the average particle charge (positive or negative)

Table 1
Number of elementary charges as function of the particle size (DBD: 9 kV, 60 Hz)

| Particle size (nm) | Number of elementary charges | | | |
|---|---|---|---|---|
| | DBD | | Corona discharge | |
| | + | − | + | − |
| 118 | 3.79 | 0.36 | 5.19 | 8.75 |
| 175 | 11.53 | 1.40 | 8.49 | 12.15 |
| 241 | 15.23 | 2.18 | 14.57 | 18.75 |

Table 2
Ratio of charged-to-total particles obtained from fluorometric analysis (DBD: 9 kV)

| | Particle size/frequency | Positively charged | Negatively charged |
|---|---|---|---|
| 60 Hz | 118 nm | 0.92 | 0.08 |
| | 175 nm | 0.83 | 0.17 |
| | 241 nm | 0.76 | 024 |
| | 514 nm | 0.61 | 0.39 |
| | 710 nm | 0.58 | 0.42 |
| 118 nm | 1 kHz | 0.69 | 0.31 |
| | 2 kHz | 0.53 | 0.47 |

at different particle sizes. The ratios were 10.4, 4.7, and 3.0 for sizes of 118, 175, and 241 nm, respectively. Table 1 also shows the particle charge data with the DC corona discharger used by Ji et al. (2004). In this study, the particle charging experiments using the corona discharger were carried out using the same applied voltage (9 kV) and face velocity (0.5 m/s) as with the DBD charger. It is interesting that although the DBD charger had asymmetric bipolar charging characteristics, its positive charging results agreed well with the results obtained from the positive DC corona discharger.

The fluorometric intensities of both positively and negatively charged particles of 118, 175, and 241 nm were measured to support the TDMA results. The ratio of charged-to-total particles was not dependent on the DBD voltage (9–11 kV) or frequency (60–120 Hz), but only on the particle size. Table 2 shows the results obtained when the DBD voltage was 9 kV. The average positive-to-negative charge ratios were calculated from the data shown in Table 2 to be 11.5, 4.9, and 3.7 for particle sizes of 118, 175, and 241 nm, which agrees well with the TDMA results. More fluorometric experiments were carried out using larger particles (514 and 710 nm) and higher frequencies (1 and 2 kHz). The positive-to-negative charge ratio approached $\sim 1$ as the particle size or frequency was increased. Stommel and Riebel (2004) reported that a high frequency AC voltage enables submicron aerosols to obtain symmetric bipolar charging (or an equilibrium charge distribution). Because of the high frequency of the fluctuating field, the particles undergo rapid charging and re-charging by positive and negative ions.

## 4. Conclusions

The charge distributions of aerosol DOS particles (118, 175, and 241 nm), charged in a DBD charger, were examined at applied voltages of 9–11 kV and frequencies of 60–120 Hz using a TDMA system. The mean number of elementary charges for the positively or negatively charged particles increased slightly with increasing applied voltage or frequency for each particle size. However, the number of elementary charges increased remarkably with increasing particle size. The charge distributions of these particles showed asymmetric bipolar charging at all applied voltages and frequencies. The positive-to-negative charge ratios for particle sizes of 118, 175, and 241 nm were 10.4, 4.7, and 3.0, respectively, at a DBD voltage and frequency of 9 kV and 60 Hz, respectively. The fluorometric data showed average positive-to-negative charge ratios to be 11.5, 4.9, and 3.7 for particle sizes of 118, 175, and 241 nm, which agreed well with the

TDMA results. More fluorometric analyses with larger particles (514 and 710 nm) and higher frequencies (1 and 2 kHz) showed that the positive-to-negative charge ratio approached unity with increasing particle size or frequency.

## Acknowledgement

This study was supported by a Seoul Development Institute (SDI) Grant (2006-8-1697).

## References

Alguacil, F. J., & Alonso, M. (2006). Multiple charging of ultrafine particles in a corona charger. *Journal of Aerosol Science*, *37*, 875–884.

Borra, J.-P. (2006). Nucleation and aerosol processing in atmospheric pressure electrical discharges: Powders production, coatings and filtration. *Journal of Physics D*, *39*, R19–R54.

Byeon, J. H., Hwang, J., Park, J. H., Yoon, K. Y., Ko, B. J., Kang, S. H. et al. (2006). Collection of submicron particles by an electrostatic precipitator using a dielectric barrier discharge. *Journal of Aerosol Science*, *37*, 1618–1628.

Dhanorkar, S., & Kamra, A. K. (2003). Effect of coagulation on the asymmetric charging of aerosols. *Atmospheric Research*, *66*, 159–173.

Duarte Fo, O. B., Marra, W. D., Jr., Kachan, G. C., & Coury, J. R. (2000). Filtration of electrified solid particles. *Industrial & Engineering Chemistry Research*, *39*, 3884–3895.

Forsyth, B., Liu, B. Y. H., & Romay, F. J. (1998). Particle charge distribution measurement for commonly generated laboratory aerosols. *Aerosol Science and Technology*, *28*, 489–501.

Hinds, W. C. (1999). *Aerosol technology: Properties, behavior, and measurement of airborne particles*. New York: Wiley.

Hoppel, A., & Frick, G. M. (1986). Ion–aerosol attachment coefficients and the steady-state charge distributions on aerosols in a bipolar ion environment. *Aerosol Science and Technology*, *12*, 471–496.

Ji, J. H., Bae, G. N., & Hwang, J. (2004). Characteristics of aerosol charge neutralizers for highly charged particles. *Journal of Aerosol Science*, *35*, 1347–1358.

Krupa, A., Jaworek, A., Lackowski, M., Czech, T., & Luckner, J. (2005). Efficiency of particle charging by an alternating electric field charger. *Journal of Electrostatics*, *63*, 673–678.

Kwon, S. B., Sakurai, H., Seto, T., & Kim, Y. J. (2006). Charge neutralization of submicron aerosols using surface-discharge microplasma. *Journal of Aerosol Science*, *37*, 483–499.

Lackowski, M., Adamiak, K., Jaworek, A., & Krupa, A. (2003). Electrostatic charging of particulates by ionic current in alternating electric field. *Powder Technology*, 135–136, 243–249.

Lackowski, M., Jaworek, A., & Krupa, A. (2003). Current–voltage characteristics of alternating electric field charger. *Journal of Electrostatics*, *58*, 77–89.

Lee, H. M., Kim, C. S., Shimada, M., & Okuyama, K. (2005). Bipolar diffusion charging for aerosol nanoparticle measurement using a soft X-ray charger. *Journal of Aerosol Science*, *36*, 813–829.

Maisels, A., Jordan, F., & Fissan, H. (2003). On the effect of charge recombination on the aerosol charge distribution in photocharging systems. *Journal of Aerosol Science*, *34*, 117–132.

Maricq, M. M. (2006). On the electrical charge of motor vehicle exhaust particles. *Journal of Aerosol Science*, *37*, 858–874.

Park, D., An, M., & Hwang, J. (2007). Development and performance test of a unipolar diffusion charger for real-time measurements of submicron aerosol particles having a log-normal size distribution. *Journal of Aerosol Science*, *38*, 420–430.

Sharma, A., & Schulman, S. G. (1999). *Introduction to fluorescence spectroscopy*. Berlin: Wiley.

Stommel, Y. G., & Riebel, U. (2004). A new corona discharge-based aerosol charger for submicron particles with low initial charge. *Journal of Aerosol Science*, *35*, 1051–1069.

Tsai, C.-J., Lin, J.-S., Deshpande, C. G., & Liu, L.-C. (2005). Electrostatic charge measurement and charge neutralization of fine aerosol particles during the generation process. *Particle & Particle Systems Characterization*, *22*, 293–298.